Does layer-specific strain using speckle tracking echocardiography improve the assessment of left ventricular myocardial deformation? A review

Yann Ancedy, Stephane Ederhy, Marie-Liesse Jean, Pascal Nhan, Laurie Soulat-Dufour, Saroumadi Adavane-Scheuble, Marion Chauvet-Droit, Franck Boccara, Ariel Cohen

HAL Id: hal-02965418

https://hal.sorbonne-universite.fr/hal-02965418

Submitted on 15 Dec 2022

Does layer-specific strain using speckle tracking echocardiography improve the assessment of left ventricular myocardial deformation? A review

Abbreviated title: Assessing LV myocardial deformation with layer-specific strain

Yann Ancedy[a], Stephane Ederhy[a], Marie-Liesse Jean[a], Pascal Nhan[a], Laurie Soulat-Dufour[a], Saroumadi Adavane-Scheuble[a], Marion Chauvet-Droit[a], Franck Boccara[a], Ariel Cohen[a,*]

[a] *Service de Cardiologie, Hôpital Saint-Antoine, AP-HP, Université Pierre-et-Marie-Curie, Paris-Sorbonne, 75571 Paris, France*

* Corresponding author at: Service de Cardiologie, Hôpital Saint-Antoine, Université Pierre et Marie Curie, Paris VI, 184 rue du Faubourg Saint-Antoine, 75571 Paris CEDEX 12, France.
E-mail address: ariel.cohen@aphp.fr (A. Cohen).

Summary

An increasing number of studies of left ventricular myocardial deformation have been published. Layer-specific strain using speckle tracking echocardiography to evaluate left ventricular function is not recommended in clinical practice. However, evaluation of myocardial mechanics using longitudinal and circumferential layer-specific strain enables the detection of subclinical impairment of myocardial deformation in various diseases. Unfortunately, normal values for longitudinal and circumferential strain have not been clearly defined. In normal subjects, layer-specific strain decreases from the endocardial to the epicardial layer, and from the apex to the base of the left ventricle. Although various studies have tried to define normal values for each layer in healthy subjects, studies with more subjects are needed. This tool has good reproducibility in terms of intraobserver and interobserver variability, but, as with monolayer strain, it has poor intervendor variability. Efforts that aim for standardization between vendors will be required before widespread use of this technique can be advocated.

Résumé

De nombreuses études concernant l'évaluation de la déformation myocardique du ventricule gauche ont été publiées. Le strain multicouche utilisant le speckle tracking pour évaluer la fonction ventriculaire gauche n'est pas recommandé en pratique clinique. Cependant, l'évaluation de la mécanique myocardique utilisant le strain multicouche longitudinal et circonférentiel a permis la détection infraclinique de l'altération de la déformation myocardique dans différentes maladies. Cependant, les valeurs normales du strain multicouche longitudinal et circonférentiel ne sont pas bien définies. Chez les sujets normaux, le strain multicouche décroit de la couche endocardique à la couche épicardique et de l'apex à la base du ventricule gauche. Bien que différentes études aient eu pour objectifs de déterminer les valeurs normales du strain de chaque couche chez les sujets normaux, des études avec de nombreux patients sont nécessaires. Cette technique a une bonne reproductibilité en terme de variabilité intra observateur et inter observateur cependant comme pour le strain monocouche, elle présente une mauvaise variabilité inter vendeur. Des efforts de standardisation sont nécessaires avant de préconiser la diffusion de cette technique.

KEYWORDS

Echocardiography;

Layer-specific strain;

Multilayer strain

Background

Layer-specific strain (LSS) using speckle tracking methodology has recently been used to try to improve myocardial deformation assessment. In contrast to monolayer strain, dedicated software measures LSS within the myocardium in three separate layers: endocardial, mid-myocardial and epicardial (Fig. 1).

The evaluation of left ventricular (LV) function using monolayer global longitudinal strain (GLS) is generally not recommended in daily clinical practice. This tool has several limitations, including intervendor variability, so it is important to standardize myocardial deformation evaluation [1]. There is also no recommendation to use LSS in clinical practice. However, an increasing number of studies have assessed this technique in various conditions.

The aims of this review were to describe data concerning normal values of longitudinal and circumferential global strain for each layer, LSS reproducibility, causes of variability and main results from studies assessing ischaemic cardiomyopathy, cardiovascular risk factors, cardiomyopathy and cardio-oncology.

Research methodology

We searched the PubMed database until June 2019 using the following algorithm: (multilayer strain[Title/Abstract] OR layer-specific[Title/Abstract]) AND echocardiography[Title/Abstract]. All articles that reported data on LSS in three layers (endocardial, mid-myocardial and epicardial) were included. We extracted data concerning normal values, reproducibility (intraobserver variability and interobserver variability, intervendor variability) and key results of studies of ischaemic cardiomyopathy, cardiovascular risk factors, cardiomyopathy and cardio-oncology.

To have homogeneous data, all studies of LSS that only considered two layers (endocardial and epicardial) were excluded. Animal studies and articles not written in English were also excluded.

Normal values

Adamu et al. [2] performed the first study that aimed to evaluate normal values of circumferential LSS in 30 normal subjects. Myocardial deformation was evaluated using the Vivid 7 system (GE Ultrasound, Horton, Norway) and LSS assessments were performed using EchoPAC software (GE

Ultrasound, Haifa, Israel). Results showed that circumferential LSS decreased from the endocardial to the epicardial layer in normal subjects (Table 1).

Leitman et al. [3] evaluated normal values of both longitudinal and circumferential LSS in 20 normal subjects. Myocardial deformation was evaluated using a Vivid 7 system (GE Vingmed Ultrasound AS, Horten, Norway) and a Vivid I system (GE Healthcare, Haifa, Israel) and LSS was assessed using EchoPAC software (GE Healthcare, Haifa, Israel). Normal values of circumferential and longitudinal LSS are presented in Table 1 and Table 2. In line with the results from Adamu et al. [2], longitudinal and circumferential LSS decreased from the endocardial to the epicardial layer [3]. Furthermore, longitudinal endocardial and mid-myocardial strain decreased from the apex to the base [3].

In a prospective study that aimed to determine reference values of both longitudinal and circumferential LSS, Shi et al. confirmed that longitudinal and circumferential LSS were highest in the apex and lowest in the base [4]. Reference values were determined in 119 healthy volunteers, echocardiography was performed on the Vivid E9 system (GE Medical Systems, Oslo, Norway) and LSS was evaluated on EchoPAC software, version BT12 (GE Vingmed, Horten, Norway). Normal values of mean GLS in endocardial, mid-myocardial and epicardial layers were $-24.3 \pm 3.1\%$, $-21.3 \pm 2.9\%$ and $-18.9 \pm 2.8\%$, respectively, and are defined from base to apex in Table 2. Normal values of mean global circumferential strain in endocardial, mid-myocardial and epicardial layers were $-34.3 \pm 4.4\%$, $-20.5 \pm 3.0\%$ and $-11.8 \pm 2.7\%$, respectively, and are defined from base to apex in Table 1.

Other studies that assessed normal LSS values are not reported in this review because only two layers were considered [5, 6].

LSS Reproducibility

Intraobserver variability

Longitudinal LSS

Table A.1 presents intraobserver variability data from studies using various different platforms and software, mainly in terms of the intraclass correlation coefficient (ICC) and the coefficient of variation [4, 7-22]. When considering longitudinal LSS of endocardial, mid-myocardial and epicardial layers, the ICCs ranged from 0.81 to 0.96, 0.85 to 0.95 and 0.82 to 0.94, respectively. Intraobserver variability using different machines and software was, therefore, satisfactory for longitudinal LSS.

Circumferential LSS

Table A.2 presents intraobserver variability data from studies using various platforms and software [2, 4, 9, 10, 12, 14, 15, 17, 18, 20-22]. When considering circumferential LSS of endocardial, mid-myocardial and epicardial layers, ICCs ranged from 0.76 to 0.96, 0.77 to 0.95 and 0.81 to 0.97, respectively. Intraobserver variability using different machines and software was, therefore, also satisfactory for circumferential LSS.

Interobserver variability

Longitudinal LSS

Table A.3 presents interobserver variability data from studies using various platforms and software [4, 7-22]. When considering longitudinal LSS of endocardial, mid-myocardial and epicardial layers, ICCs ranged from 0.85 to 0.96, 0.85 to 0.94 and 0.81 to 0.93, respectively.

Circumferential LSS

Table A.4 presents interobserver variability data from studies using various platforms and software [2, 4, 9, 10, 12, 14, 15, 17, 18, 20-22]. When considering circumferential LSS of endocardial, mid-myocardial and epicardial layers, ICCs ranged from 0.71 to 0.93, 0.65 to 0.92 and 0.73 to 0.92, respectively.

Causes of LSS variability

Determinants of LV longitudinal and circumferential LSS in 119 healthy subjects have been reported to be sex, heart rate and stroke volume for endocardial, mid-myocardial and epicardial GLS; whereas only heart rate independently predicted endocardial, mid-myocardial and epicardial global circumferential strain [4]

When considering aging, a study by Abou et al. showed that the magnitude of LV longitudinal strain at the basal level declined, whereas the apical LV longitudinal strain increased. However, a layer-specific LV longitudinal strain remained unchanged with aging. The presence of diabetes

mellitus modulated the effect of age on the LV endocardial layer, and male sex was associated with more impaired longitudinal strain at the epicardial layer [23].

As with monolayer strain, intervendor variability is a major cause of variability in LSS. In a previous study, we investigated intervendor variability between Vivid E9 (General Electric, Fairfield, CT, USA) and ACUSON SC2000 (Siemens, Munich, Germany). Our results showed poor agreement for LSS evaluation between the two platforms using their dedicated software for LSS assessment [24]. Therefore, we concluded that patients should be followed using the same platform. Moreover, when comparing endocardial and mid-myocardial GLS between five vendors (GE, Hitachi, Siemens, Toshiba and TomTec), measurements showed that intervendor bias was higher for mid-myocardial GLS compared with endocardial GLS [25].

Physiology and specific factors influencing layer strain differences

Differences in layer-specific strain values could be explain by human heart distribution of fibres that present various angles. Fibre distribution has angles varying from about 60° (in circumferential plane) at the inner surface to about –60° at the outer surface. The ratio of circumferentially to longitudinally oriented fibres is 10:1, increasing from the apex to the base [3]. Other studies performed on animal models have shown that fibres vary transmurally from approximately –70° in the epicardial layer to +80° in the endocardial layer [26, 27].

Furthermore, the pattern of myocardial fibre shortening and thickening varies according to the layer. The endocardial layer undergoes greater dimensional changes (both thickening and shortening) during systole than the epicardial layer. A study by Sabbah et al. revealed that the endocardial layer of the LV wall accounted for 83% of wall thickening during diastole. The endocardial layer shortened by 18% during systole, whereas the epicardial layer shortened by only 10%. A 22% reduction in the internal LV diameter was observed, whereas only a 6% reduction in the external diameter occurred during systole. The same results were found for LV internal and external volumes [28].

Main indications assessed using LSS

Table 3 summarizes results from the main topics assessed using speckle tracking LSS.

Ischaemic cardiomyopathy

Adamu et al. [2] were the first to demonstrate that myocardial deformation was significantly reduced in all layers of segments with impaired wall motion compared with normokinetic segments in 20 patients with ischaemic cardiomyopathy.

Detection of myocardial ischaemia using stress echocardiography (dobutamine or adenosine) and LSS is feasible in patients with coronary artery disease (CAD) [8, 29]. Park et al. [29] showed that endocardial GLS during recovery is a sensitive variable for CAD identification (cut-off: –16%). Additional evaluation of endocardial GLS improved the diagnostic accuracy of dobutamine stress echocardiography compared with standard dobutamine stress echocardiography evaluation. Moreover, endocardial GLS during recovery correlated with all-cause mortality [29]. Furthermore, identifying LSS in dipyridamole stress echocardiography showed that global circumferential strain could be used to distinguish microvascular disease, and that endocardial GLS was the best indicator of an altered wall deformation associated with macrovascular ischaemia [30].

Furthermore, studies have shown that, in patients with chest pain suspected to be CAD, LSS assessment enabled the detection of non-ST-segment elevation acute coronary syndrome (NSTE-ACS) [15, 31]. Sarvari et al. [15] demonstrated that assessment of endocardial and mid-myocardial territorial longitudinal strain echocardiography (calculated according to the perfusion territories of the three major coronary arteries in a 16-segment LV model by LSS) provided higher accuracy than epicardial strain ($P < 0.05$), Wall Motion Score Index ($P < 0.01$) or ejection fraction ($P < 0.001$) for the identification of patients with NSTE-ACS and significant CAD. Endocardial function was more affected in patients with significant CAD compared with epicardial function [15]. Zhang et al. [31] confirmed these results, showing that assessment of LSS, especially endocardial strain, could identify patients with NSTE-ACS and complex CAD, and could predict the severity of coronary lesions. Liu et al. [13] showed that evaluation of regional longitudinal strain by LSS at rest can be used to screen for significant stenosis of the left anterior descending artery in patients with suspected NSTE-ACS. Endocardial regional longitudinal strain of the left anterior descending artery was the only predictor of significant stenosis of this artery, without recourse to all other routine echocardiographic predictors and baseline clinical data [13]. In addition, strain echocardiography can be carried out at the bedside in the emergency setting. Therefore, LSS could be a non-invasive tool to rapidly identify patients with suspected NSTE-ACS who would benefit from reperfusion therapy [13].

Moreover, LSS can be used to identify transmural and non-transmural infarction. In a study that included 138 patients with LV chronic ischaemic cardiomyopathy, Becker et al. [32]. reported that non-transmural infarction resulted in greater impairment of myocardial deformation of the endocardial than the epicardial myocardial layer. In transmural infarction, deformation of the endocardial and epicardial myocardial layers is impaired similarly. A layer-specific analysis of myocardial deformation allows accurate discrimination between different transmurality categories of myocardial infarction, and appears to be superior to total wall thickness myocardial deformation analysis, as determined using monolayer strain [32]. Nevertheless, a more recent study demonstrated that combining longitudinal LSS measurements does not provide additional information for detection of regional functional abnormalities. When comparing four vendors (GE, Siemens, Toshiba and TomTec), both endocardial and mid-wall strain values were decreased in scarred segments. Endocardial and mid-wall strain variables showed no difference in scar detection capability [33].

LSS can be used to assess myocardial viability in patients having a myocardial infarction, but is not superior to monolayer strain assessment using single-photon emission computed tomography (SPECT) [34]. In 47 patients who were evaluated for myocardial viability, a cut-off value of –6.5% for mid-myocardial longitudinal strain had a sensitivity of 76% and a specificity of 76% to predict segmental myocardial viability [34]. However, Liu et al. [13] reported different data, showing that endocardial LSS and endocardial LSS rate analysis are relevant for the assessment of myocardial viability. Their sensitivity, specificity and accuracy for the evaluation of myocardial viability were 77.1%, 65.4% and 72.9% for endocardial LSS, and 72.9%, 65.4% and 69.7% for endocardial LSS, respectively. Moreover, parallel and serial tests of combinations of endocardial LSS and endocardial LSS rate showed similar sensitivity, specificity and accuracy to dual isotope simultaneous acquisition SPECT for this indication [35].

Cardiovascular risk factors

Hypertension contributes to decreased myocardial deformation [11, 20]. LSS enables the detection of subclinical myocardial impairment in patients with hypertension [11]. Kim et al. showed that longitudinal LSS measurements of patients with hypertension were significantly lower than those of normotensive controls in all three LV layers [11].

Myocardial deformation impairment may be differentiated according to the cause of hypertension. Wang et al. compared longitudinal and circumferential LSS in patients treated for aldosterone-producing adenoma, idiopathic hyperaldosteronism and primary hypertension. Results revealed that patients with primary aldosteronism, especially aldosterone-producing adenoma, had impaired regional systolic function with myocardial deformation changes at similar levels of blood pressure, probably because of elevated plasma aldosterone concentration [36]. A study that compared longitudinal LSS and circumferential LSS in 48 patients with diabetes, 54 patients with diabetes and hypertension and 44 controls revealed that diabetes and hypertension significantly affected LV deformation assessed by monolayer strain and LSS [18]. Further, hypertension had an additional negative effect on LV deformation in patients with diabetes [18]. Fasting glucose and glycated haemoglobin levels have also been associated with LV mechanics evaluated by comprehensive two-dimensional strain analysis, independent of LV structure and diastolic function [18]. Moreover, acute hyperglycaemia impairs systolic LV myocardial mechanics in asymptomatic patients with diabetes, by reducing longitudinal and circumferential LSS. A study that included normotensive patients with uncomplicated diabetes, with acute hyperglycaemia (≥ 11.1 mmol/L) or with optimal metabolic control (fasting plasma glucose < 7 mmol/l and glycated haemoglobin < 7%), and 20 healthy individuals who served as controls revealed that alteration of myocardial deformation assessed by LSS was not reversible after 3 months of good glycaemic control [37]. Apart from hyperglycaemia, duration of diabetes has an influence on longitudinal and circumferential LSS. These results were demonstrated in type 1 diabetes mellitus. In fact, longitudinal deformation in all layers and epicardial and mid-myocardial circumferential deformation at the basal level decreased from the late teens, and longitudinal and circumferential LSS values were correlated with disease duration and LV hypertrophy [38].

Hypercholesterolaemia also contributes to impaired myocardial deformation when assessed using LSS [12]. Layer-specific LV evaluation has great value for assessing early impairment of LV function in patients with familial hypercholesterolaemia. In a study that compared 49 patients with heterozygous familial hypercholesterolaemia with 32 controls, Leng et al. [12] demonstrated that longitudinal strain of the endocardium and mid-myocardium were significantly reduced in patients with heterozygous familial hypercholesterolaemia (both $P < 0.001$). In LSS circumferential strain, only the circumferential strain of the endocardium was significantly reduced ($P < 0.001$). The degree of strain

reduction was positively correlated with total cholesterol and low-density lipoprotein cholesterol concentrations [12].

Cardiomyopathy

Myocardial deformation is impaired in patients with hypertrophic cardiomyopathy [14]. A study that compared longitudinal LSS in 41 patients with hypertrophic cardiomyopathy and 27 control subjects demonstrated that patients with hypertrophic cardiomyopathy had significantly lower longitudinal LSS for each layer compared with controls [14]. However, circumferential LSS was impaired in the mid-myocardial and epicardial layers, but was preserved in the endocardial layer. Preserved circumferential endocardial layer function was also correlated with a normal LV ejection fraction [14]. In addition, Sun et al. [17] demonstrated that patients with hypertrophic cardiomyopathy had marked reductions in longitudinal and circumferential LSS, whereas patients with hypertensive LV hypertrophy had smaller reductions in longitudinal LSS and preserved circumferential LSS [17]. Furthermore, when considering the treatment of obstructive hypertrophic cardiomyopathy using alcohol septal ablation, Zhang et al. [39] showed an increased specific longitudinal LSS in the endocardium, especially in the basal septum, which may be a valid marker of echocardiographic improvement in patients with obstructive hypertrophic cardiomyopathy receiving alcohol septal ablation.

It is difficult to distinguish LV non-compaction from dilated cardiomyopathy, but longitudinal LSS could help to provide criteria that could confirm the diagnosis of LV non-compaction. In a study that compared 48 patients with LV non-compaction with 45 who had dilated cardiomyopathy using LSS, Tarando et al. [40] showed that myocardial deformations appear to be informative for distinguishing idiopathic dilated cardiomyopathy from LV non-compaction. The authors reported a base-apex gradient that identified significantly more marked apical deformations in patients with LV non-compaction [40].

Cardio-oncology

Longitudinal and circumferential LSS may be useful for the detection of subclinical LV dysfunction in patients treated with anthracycline. In a study that included 42 anthracycline-treated survivors of large B-cell non-Hodgkin lymphoma, Kang et al. [10] showed that there was preferential impairment of subendocardial deformation in long-term survivors after exposure to anthracycline. LSS allowed the

detection of subclinical anthracycline-induced myocardial abnormalities [10].

These results were confirmed by a study that evaluated 56 patients treated with anthracycline for childhood cancer [22]. This study demonstrated that impairment of endocardial circumferential deformation in adolescent patients was the initial cardiac abnormality in those who had survived childhood cancer treated with anthracycline. Further, this impairment extended from the endocardial towards the epicardial layer and from the base towards the apex with age [22].

Conclusions

Evaluation of myocardial mechanics using longitudinal and circumferential LSS enables the detection of early impairment of myocardial deformation in several medical conditions. In normal subjects, LSS decreases from the endocardial to the epicardial layer and from the apex to the base of the left ventricle. Although several studies have aimed to define normal values of each layer in healthy subjects, studies with more subjects are needed. Although this tool has good reproducibility in terms of intraobserver and interobserver variability, like monolayer strain analysis, it suffers from intervendor variability (Central illustration). Efforts to achieve standardization between vendors would therefore be required before the widespread use of this technique could be advocated.

References

[1]   Voigt JU, Pedrizzetti G, Lysyansky P, et al. Definitions for a common standard for 2D speckle tracking echocardiography: consensus document of the EACVI/ASE/Industry Task Force to standardize deformation imaging. Eur Heart J Cardiovasc Imaging 2015;16:1-11.

[2]   Adamu U, Schmitz F, Becker M, Kelm M, Hoffmann R. Advanced speckle tracking echocardiography allowing a three-myocardial layer-specific analysis of deformation parameters. Eur J Echocardiogr 2009;10:303-8.

[3]   Leitman M, Lysiansky M, Lysyansky P, et al. Circumferential and longitudinal strain in 3 myocardial layers in normal subjects and in patients with regional left ventricular dysfunction. J Am Soc Echocardiogr 2010;23:64-70.

[4]   Shi J, Pan C, Kong D, Cheng L, Shu X. Left Ventricular Longitudinal and Circumferential Layer-Specific Myocardial Strains and Their Determinants in Healthy Subjects. Echocardiography 2016;33:510-8.

[5]   Alcidi GM, Esposito R, Evola V, et al. Normal reference values of multilayer longitudinal strain according to age decades in a healthy population: A single-centre experience. Eur Heart J Cardiovasc Imaging 2018;19:1390-6.

[6]   Nagata Y, Wu VC, Otsuji Y, Takeuchi M. Normal range of myocardial layer-specific strain using two-dimensional speckle tracking echocardiography. PLoS One 2017;12:e0180584.

[7]   Cong J, Wang Z, Jin H, et al. Quantitative evaluation of longitudinal strain in layer-specific myocardium during normal pregnancy in China. Cardiovasc Ultrasound 2016;14:45.

[8]   Ejlersen JA, Poulsen SH, Mortensen J, May O. Diagnostic value of layer-specific global longitudinal strain during adenosine stress in patients suspected of coronary artery disease. Int J Cardiovasc Imaging 2017;33:473-80.

[9]   Hamada S, Schroeder J, Hoffmann R, et al. Prediction of Outcomes in Patients with Chronic Ischemic Cardiomyopathy by Layer-Specific Strain Echocardiography: A Proof of Concept. J Am Soc Echocardiogr 2016;29:412-20.

[10]   Kang Y, Xiao F, Chen H, et al. Subclinical Anthracycline-Induced Cardiotoxicity in the Long-Term Follow-Up of Lymphoma Survivors: A Multi-Layer Speckle Tracking Analysis. Arq Bras Cardiol 2018;110:219-28.

[11]   Kim SA, Park SM, Kim MN, Shim WJ. Assessment of Left Ventricular Function by Layer-Specific Strain and Its Relationship to Structural Remodelling in Patients With Hypertension. Can J Cardiol 2016;32:211-6.

[12]   Leng Z, Li R, Li Y, Wang L, Wang Y, Yang Y. Myocardial layer-specific analysis in patients with heterozygous familial hypercholesterolemia using speckle tracking echocardiography. Echocardiography 2017;34:390-6.

[13]   Liu C, Li J, Ren M, et al. Multilayer longitudinal strain at rest may help to predict significant stenosis of the left anterior descending coronary artery in patients with suspected non-ST-elevation acute coronary syndrome. Int J Cardiovasc Imaging 2016;32:1675-85.

[14]   Okada K, Yamada S, Iwano H, et al. Myocardial shortening in 3 orthogonal directions and its transmural variation in patients with nonobstructive hypertrophic cardiomyopathy. Circ J 2015;79:2471-9.

[15]   Sarvari SI, Haugaa KH, Zahid W, et al. Layer-specific quantification of myocardial deformation by strain echocardiography may reveal significant CAD in patients with non-ST-segment elevation acute coronary syndrome. JACC Cardiovasc Imaging 2013;6:535-44.

[16]   Shiino K, Yamada A, Scalia GM, et al. Early Changes of Myocardial Function After Transcatheter Aortic Valve Implantation Using Multilayer Strain Speckle Tracking Echocardiography. Am J Cardiol 2019;123:956-60.

[17]   Sun JP, Xu TY, Ni XD, et al. Echocardiographic strain in hypertrophic cardiomyopathy and hypertensive left ventricular hypertrophy. Echocardiography 2019;36:257-65.

[18]   Tadic M, Cuspidi C, Vukomanovic V, et al. Layer-specific deformation of the left ventricle in uncomplicated patients with type 2 diabetes and arterial hypertension. Arch Cardiovasc Dis 2018;111:17-24.

[19]   Wang Y, Ma C, Zhang Y, et al. Layer-specific analysis of left ventricular myocardial contractility in patients with coronary slow-flow phenomenon. J Clin Ultrasound 2016;44:429-36.

[20]   Xu L, Wang N, Chen X, Liang Y, Zhou H, Yan J. Quantitative evaluation of myocardial layer-specific strain using two-dimensional speckle tracking echocardiography among young adults with essential hypertension in China. Medicine (Baltimore) 2018;97:e12448.

[21]   Yamada M, Takahashi K, Kobayashi M, et al. Mechanisms of Left Ventricular Dysfunction

         Assessed by Layer-Specific Strain Analysis in Patients With Repaired Tetralogy of Fallot. Circ

         J 2017;81:846-54.

[22]   Yazaki K, Takahashi K, Shigemitsu S, et al. In-Depth Insight Into the Mechanisms of Cardiac

         Dysfunction in Patients With Childhood Cancer After Anthracycline Treatment Using Layer-

         Specific Strain Analysis. Circ J 2018;82:715-23.

[23]   Abou R, Leung M, Khidir MJH, et al. Influence of Aging on Level and Layer-Specific Left

         Ventricular Longitudinal Strain in Subjects Without Structural Heart Disease. Am J Cardiol

         2017;120:2065-72.

[24]   Ancedy Y, Ederhy S, Lang S, et al. Multilayer global longitudinal strain in patients with cancer:

         A comparison of two vendors. Arch Cardiovasc Dis 2018;111:285-96.

[25]   Unlu S, Mirea O, Duchenne J, et al. Comparison of Feasibility, Accuracy, and Reproducibility

         of Layer-Specific Global Longitudinal Strain Measurements Among Five Different Vendors: A

         Report from the EACVI-ASE Strain Standardization Task Force. J Am Soc Echocardiogr

         2018;31:374-80 e1.

[26]   Arts T, Costa KD, Covell JW, McCulloch AD. Relating myocardial laminar architecture to shear

         strain and muscle fiber orientation. Am J Physiol Heart Circ Physiol 2001;280:H2222-9.

[27]   Geerts L, Bovendeerd P, Nicolay K, Arts T. Characterization of the normal cardiac myofiber

         field in goat measured with MR-diffusion tensor imaging. Am J Physiol Heart Circ Physiol

         2002;283:H139-45.

[28]   Sabbah HN, Marzilli M, Stein PD. The relative role of subendocardium and subepicardium in

         left ventricular mechanics. Am J Physiol 1981;240:H920-6.

[29]   Park JH, Woo JS, Ju S, et al. Layer-specific analysis of dobutamine stress echocardiography

         for the evaluation of coronary artery disease. Medicine (Baltimore) 2016;95:e4549.

[30]   Mandoli GE, Cameli M, Minardi S, Crudele F, Lunghetti S, Mondillo S. Layer-specific strain in

         dipyridamole stress echo: A new tool for the diagnosis of microvascular angina.

         Echocardiography 2018;35:2005-13.

[31]   Zhang L, Wu WC, Ma H, Wang H. Usefulness of layer-specific strain for identifying complex

         CAD and predicting the severity of coronary lesions in patients with non-ST-segment elevation

         acute coronary syndrome: Compared with Syntax score. Int J Cardiol 2016;223:1045-52.

[32] Becker M, Ocklenburg C, Altiok E, et al. Impact of infarct transmurality on layer-specific impairment of myocardial function: a myocardial deformation imaging study. Eur Heart J 2009;30:1467-76.

[33] Unlu S, Mirea O, Pagourelias ED, et al. Layer-Specific Segmental Longitudinal Strain Measurements: Capability of Detecting Myocardial Scar and Differences in Feasibility, Accuracy, and Reproducibility, Among Four Vendors A Report From the EACVI-ASE Strain Standardization Task Force. J Am Soc Echocardiogr 2019;32:624-32 e11.

[34] Orloff E, Fournier P, Bouisset F, et al. Myocardial multilayer strain does not provide additional value for detection of myocardial viability assessed by SPECT imaging over and beyond standard strain. Echocardiography 2018;35:1300-9.

[35] Liu K, Wang Y, Hao Q, Li G, Chen P, Li D. Evaluation of myocardial viability in patients with acute myocardial infarction: Layer-specific analysis of 2-dimensional speckle tracking echocardiography. Medicine (Baltimore) 2019;98:e13959.

[36] Wang D, Xu JZ, Chen X, et al. Speckle-Tracking Echocardiographic Layer-Specific Strain Analysis on Subclinical Left Ventricular Dysfunction in Patients With Primary Aldosteronism. Am J Hypertens 2019;32:155-62.

[37] Bogdanovic J, Asanin M, Krljanac G, et al. Impact of acute hyperglycemia on layer-specific left ventricular strain in asymptomatic diabetic patients: an analysis based on two-dimensional speckle tracking echocardiography. Cardiovasc Diabetol 2019;18:68.

[38] Iso T, Takahashi K, Yazaki K, et al. In-Depth Insight Into the Mechanisms of Cardiac Dysfunction in Patients With Type 1 Diabetes Mellitus Using Layer-Specific Strain Analysis. Circ J 2019;83:1330-7.

[39] Zhang J, Zhu L, Jiang X, Hu Z. Layer-specific strain analysis of left ventricular myocardium after alcohol septal ablation for hypertrophic obstructive cardiomyopathy. Medicine (Baltimore) 2018;97:e13083.

[40] Tarando F, Coisne D, Galli E, et al. Left ventricular non-compaction and idiopathic dilated cardiomyopathy: the significant diagnostic value of longitudinal strain. Int J Cardiovasc Imaging 2017;33:83-95.

[41]   Shi J, Xing Y, Qian J, et al. Early Assessment of Left Ventricular Function by Layer-Specific Strain and Its Relationship to Pulsatile Arterial Load in Patients with Coronary Slow Flow. Int Heart J 2019;60:586-92.

Figure legends

Figure 1. Layer-specific global longitudinal strain of endocardial (GSendo), mid-myocardial (SG), and epicardial (GSepi) layers.

Central illustration. Layer-specific strain characteristics using speckle tracking. 2D: two-dimensional; ICC: intraclass correlation coefficient; LSS: layer-specific strain; LV: left ventricle.

Table 1 Circumferential layer-specific strain in normal subjects.

Study	n	Machine	Software	Endo base	Endo mid-ventricle	Endo apex	Mid base	Mid mid-ventricle	Mid apex	Epi base	Epi mid-ventricle	Epi apex
Adamu et al. 2008 [2]	30	Vivid 7[a]	EchoPAC[e]	36.4 ± 8.2	37.9 ± 7.9	39.9 ± 9.2	27.7 ± 7.9	29.1 ± 7.4	29.8 ± 9.7	23.2 ± 9.8	23.8 ± 6.8	24.9 ± 8.9
Leitman et al. 2010 [3]	20	Vivid 7[b] or Vivid I[c]	EchoPAC[c]	−32.4 ± 8.4	−35.5 ± 9.1	−44.2 ± 11.2	−22.2 ± 8.0	−26.8 ± 6.1	−34.0 ± 4.9	−15.6 ± 6.7	−19.9 ± 6.4	−26.1 ± 7.6
Shi et al. 2016 [4]	119	Vivid E9[d]	EchoPAC, v BT12[f]	−30.22 ± 4.76	−32.50 ± 5.94	−39.71 ± 8.18	−19.19 ± 2.90	−20.74 ± 3.87	−24.39 ± 4.82	−11.33 ± 2.77	−12.61 ± 3.44	−15.81 ± 4.33

Data are expressed as mean ± standard deviation. Endo: endocardial; Epi: epicardial; Mid: mid-myocardial; v: version.

[a] GE Ultrasound, Horton, Norway.

[b] GE Vingmed Ultrasound AS, Horten, Norway.

[c] GE Healthcare, Haifa, Israel.

[d] GE Medical Systems, Oslo, Norway.

[e] GE Ultrasound, Haifa, Israel.

[f] GE Vingmed, Horten, Norway.

Table 2 Longitudinal layer-specific strain in normal subjects.

Study	*n*	Machine	Software	Endo base	Endo mid-ventricle	Endo apex	Mid base	Mid mid-ventricle	Mid apex	Epi base	Epi mid-ventricle	Epi apex
Leitman et al. 2010 [3]	20	Vivid 7[a] or Vivid I	EchoPAC[b]	−20.3 ± 4.8	−23.5 ± 3.6	−33.5 ± 5.3	−19.8 ± 3.2	−21.3 ± 3.1	−25.0 ± 4.5	−19.2 ± 3.2	−19.4 ± 3.0	−18.9 ± 3.9
Shi et al. 2016 [4]	119	Vivid E9[c]	EchoPAC, v BT12[d]	−19.16 ± 4.01	−22.41 ± 3.59	−28.11 ± 3.70	−18.38 ± 3.01	−20.48 ± 2.97	−25.70 ± 3.95	−17.76 ± 2.72	−18.87 ± 2.83	−20.07 ± 3.70

Data are expressed as mean ± standard deviation. Endo: endocardial; Epi: epicardial; Mid: mid-myocardial; v: version.

[a] GE Vingmed Ultrasound AS, Horten, Norway.

[b] GE Healthcare, Haifa, Israel.

[c] GE Medical Systems, Oslo, Norway.

[d] GE Vingmed, Horten, Norway.

Table 3 Layer-specific strain in various cardiac diseases.

	Endo GLS	Mid GLS	Epi GLS	Endo GCS	Mid GCS	Epi GCS
Coronary artery disease						
Detection of myocardial ischaemia using stress echocardiography [8, 29]	⇓⇓	⇓	⇓	ND	ND	ND
Transmural infarction	⇓	⇓	⇓	⇓	⇓	⇓
Non-transmural infarction [2, 25, 32]				⇓⇓	⇓	⇓
NSTE-ACS [15]	⇓⇓	⇓⇓	⇓	ND	ND	ND
Cardiovascular risk factors						
Hypertension [11, 20]	⇓⇓	⇓⇓	⇓	ND	ND	ND
Diabetes [37, 38]	⇓	⇓	⇓	⇓	⇓	⇓
Hypercholesterolaemia [12]	⇓⇓	⇓⇓	-	⇓⇓	-	-
Cardiomyopathy						
Hypertrophic cardiomyopathy [14, 17]	⇓	⇓	⇓	⇓	⇓	⇓
Cardio-oncology						
Detection of subclinical LV dysfunction in patients treated with anthracycline [10, 22]	⇓⇓	⇓	⇓	⇓⇓	⇓	⇓

Endo: endocardial; Epi: epicardial; GLS: global longitudinal strain; LV: left ventricular; Mid: mid-myocardial; ND: not defined; NSTE-ACS: non-ST segment elevation acute coronary syndrome.

Appendix

Table A.1   Intraobserver variability in longitudinal layer-specific strain.

Study	*n*	Ultrasound machine; vendor	Software; vendor	Intraobserver variability
Shi et al. 2019 [41]	20	Vivid E9; GE Medical Systems, Oslo, Norway	EchoPAC, v 201.x.x; GE Vingmed, Horten, Norway	Endo CV: 5.4 Mid CV: 5.4 Epi CV: 6.2
Iso et al. 2019 [38]	12	Vivid E9; GE Healthcare, Milwaukee, WI, USA	EchoPAC, v 113.1.0 GE Vingmed Ultrasound AS, Horten, Norway	Endo CV: 4.87 Mid CV: 6.40 Epi CV: 8.46
Shiino et al. 2019 [16]	20	Vivid E95; GE Healthcare, Horten, Norway EPIQ; Philips, Amsterdam, Netherlands ACUSON SC2000; Siemens Medical Solutions, Malvern, PA, USA	TomTec; TomTec Imaging Systems, Unterschleissheim, Germany	Endo ICC: 0.93 Mid ICC: 0.89 Epi ICC: 0.85
Sun et al. 2019 [17]	20	Vivid E9; GE Healthcare, Horten, Norway	EchoPAC PC, v 113.0.5; GE Healthcare	Endo ICC: 0.94 Mid ICC: 0.94 Epi ICC: 0.89

Xu et al. 2018 [20]	NA	Vivid E9; GE Healthcare, Horten, Norway	EchoPAC PC, v 113.0.5 GE Healthcare	Endo ICC: 0.81 Mid ICC: 0.89 Epi ICC: 0.94
Kang et al. 2018 [10]	10	Vivid E9; GE Healthcare, Horten, Norway	EchoPAC, v 11.1; GE Healthcare, Horten, Norway	Endo ICC: 0.86 Mid ICC: 0.85 Epi ICC: 0.82
Yazaki et al. 2018 [22]	12	Vivid E9; GE Healthcare, Milwaukee, WI, USA	EchoPAC, v 113.1.0; GE Vingmed Ultrasound AS, Horten, Norway	Endo CV: 3.62 Mid CV: 1.93 Epi CV: 3.65
Tadic et al. 2018 [18]	20	Vivid 7; GE Vingmed, Horten, Norway	EchoPAC, v 201; GE Healthcare, Horten, Norway	Endo ICC: 0.932 Mid ICC: 0.927 Epi ICC: 0.852
Yamada et al. 2017 [21]	10	Vivid E7/Vivid E9; GE Healthcare, Milwaukee, WI, USA	EchoPAC, v 113.1.0; GE Vingmed Ultrasound AS, Horten, Norway	Endo CV: 2.07 Mid CV: 1.93 Epi CV: 1.93
Leng et al. 2017 [12]	32	Vivid 7; GE Healthcare, Horten, Norway	EchoPAC Dimension '08; GE Healthcare	Endo ICC: 0.882 Mid ICC: 0.901 Epi ICC: 0.821
Ejlersen et al.	20	Vivid 7;	EchoPAC, v 113;	Endo MOD ± 95% LOA: 0.27 ± 1.72

Study	N	Ultrasound system	Software	Results
2017 [8]		GE Healthcare, Horten, Norway	GE Vingmed Ultrasound AS, Horten, Norway	Mid MOD ± 95% LOA: 0.20 ± 1.63
				Epi MOD ± 95% LOA: 0.10 ± 1.68
Cong et al.	NA	Vivid E9;	EchoPAC PC, v 113.1.0	Endo MPE[a]: 11.7%
			GE Vingmed Ultrasound AS, Horten, Norway	
2016 [7]		GE Healthcare, Horten, Norway		Mid MPE[a]: 12.3%
				Epi MPE[a]: 12.4%
Hamada et al.	40	Vivid 7/Vivid E9;	EchoPAC, v 113.1.0;	Endo ICC: 0.91
2016 [9]		GE Vingmed Ultrasound AS, Horten, Norway	GE Vingmed Ultrasound AS, Horten, Norway	
Kim et al.	10	ACUSON SC2000;	Syngo SC2000 Workplace, v 3.0;	Endo ICC: 0.953
2016 [11]		Siemens Medical Solutions, Malvern, PA, USA	Siemens Medical Solutions, Malvern, PA, USA	Mid ICC: 0.953
				Epi ICC: 0.828
Shi et al.	20	Vivid E9;	EchoPAC, v BT12;	Endo CV ± SD: 5.4 ± 4.5
2016 [4]		GE Medical Systems, Oslo, Norway	GE Vingmed, Horten, Norway	Mid CV ± SD: 5.4 ± 4.6
				Epi CV ± SD: 6.2 ± 4.3
Wang et al.	10	Vivid 7;	EchoPAC, v 11.3;	Endo MOD (95% CI): 0.51% (−1.18 to 0.82%)
2016 [19]		GE Healthcare, Waukesha, WI, USA	GE Healthcare	Mid MOD (95% CI): 0.38% (−0.89 to 0.59%)
				Epi MOD (95% CI): 0.45% (−1.01 to 0.77%)

Liu et al.	15	Vivid E9;	EchoPAC, v 113;	Endo ICC: 0.92	
2016 [13]		GE Healthcare, Horten, Norway	GE Healthcare, Horten, Norway	Mid ICC: 0.90	
				Epi ICC: 0.92	
Okada et al.	15	Artida;	Artida built-in software;	Endo VV: 7%	
2015 [14]		Toshiba Medical Systems, Tochigi, Japan	Toshiba Medical Systems, Tochigi, Japan	Mid VV: 8%	
				Epi VV: 13%	
Sarvari et al.	10	Artida;	Artida built-in software;	Endo ICC: 0.96	
2013 [15]		Toshiba Medical Systems, Tochigi, Japan	Toshiba Medical Systems, Tochigi, Japan	Mid ICC: 0.87	
				Epi ICC: 0.94	

CI: confidence interval; CV: coefficient of variation; Endo: endocardial; Epi: epicardial; ICC: intraclass correlation coefficient; LOA: limits of agreement; MD: mean difference; Mid: mid-myocardial; MOD: mean of differences; MPE: mean percentage error; NA: not available; SD: standard deviation; v: version; VV: variability value.

[a] Absolute difference divided by the mean of the two observations.

Table A.2   Intraobserver variability in circumferential layer-specific strain.

Study	n	Ultrasound machine; vendor	Software; vendor	Intraobserver variability
Shi et al. 2019 [41]	20	Vivid E9; GE Medical Systems, Oslo, Norway	EchoPAC, v 201.x.x; GE Vingmed, Horten, Norway	Endo CV: 6.2 Mid CV: 9.0 Epi CV: 8.6
Iso et al. 2019 [38]	12	Vivid E9; GE Healthcare, Milwaukee, WI, USA	EchoPAC, v 113.1.0; GE Vingmed Ultrasound AS, Horton, Norway	Endo basal CV: 4.31 Mid basal CV: 3.57 Epi basal CV: 5.25 Endo papillary CV: 3.49 Mid papillary CV: 3.60 Epi papillary CV: 6.62 Endo apical CV: 4.88 Mid apical CV: 4.28 Epi apical CV: 8.18
Sun et al. 2019 [17]	20	Vivid E9; GE Healthcare, Horten, Norway	EchoPAC PC, v 113.0.5; GE Healthcare	Endo ICC: 0.92 Mid ICC: 0.92 Epi ICC: 0.93
Xu et al.	NA	Vivid E9;	EchoPAC PC, v 113.0.5;	Endo ICC: 0.76

2018 [20]		GE Healthcare, Horten, Norway	GE Healthcare	Mid ICC: 0.77
				Epi ICC: 0.81
Kang et al.	10	Vivid E9;	EchoPAC, v 11.1;	Endo ICC: 0.96
2018 [10]		GE Healthcare, Horton, Norway	GE Healthcare, Horton, Norway	Mid ICC: 0.89
				Epi ICC: 0.97
Yazaki et al.	12	Vivid E9;	EchoPAC, v 113.1.0;	Endo basal CV: 2.90
2018 [22]		GE Healthcare, Milwaukee, WI, USA	GE Vingmed Ultrasound AS, Horton, Norway	Mid basal CV: 2.52
				Epi basal CV: 7.82
				Endo papillary CV: 2.77
				Mid papillary CV: 3.75
				Epi papillary CV: 9.03
				Endo apical CV: 3.30
				Mid apical CV: 8.88
				Epi apical CV: 8.79
Tadic et al.	20	Vivid 7;	EchoPAC, v 201;	Endo ICC: 0.920
2018 [18]		GE Vingmed, Horten, Norway	GE Healthcare, Horten, Norway	Mid ICC: 0.929
				Epi ICC: 0.836
Yamada et al.	10	Vivid E7/Vivid E9;	EchoPAC, v 113.1.0;	Endo basal CV: 1.83
2017 [21]		GE Healthcare, Milwaukee, WI, USA	GE Vingmed Ultrasound AS, Horton, Norway	Mid basal CV: 2.52

				Epi basal CV: 2.90
				Endo papillary CV: 2.90
				Mid papillary CV: 3.75
				Epi papillary CV: 5.78
				Endo apical CV: 10.2
				Mid apical CV: 8.88
				Epi apical CV: 8.96
Leng et al. 2017 [12]	32	Vivid 7; GE Healthcare, Horten, Norway	EchoPAC Dimension 08; GE Healthcare	Endo ICC: 0.919 Mid ICC: 0.953 Epi ICC: 0.822
Hamada et al. 2016 [9]	40	Vivid 7/Vivid E9; GE Vingmed Ultrasound AS, Horten, Norway	EchoPAC, v 113.1.0; GE Vingmed Ultrasound AS, Horten, Norway	Endo ICC: 0.91
Shi et al. 2016 [4]	20	Vivid E9; GE Medical Systems, Oslo, Norway	EchoPAC, v BT12; GE Vingmed, Horten, Norway	Endo CV ± SD: 6.2 ± 3.7 Mid CV ± SD: 9.0 ± 1.0 Epi CV ± SD: 8.6 ± 5.0
Okada et al. 2015 [14]	15	Artida; Toshiba Medical Systems, Tochigi, Japan	Artida built-in software; Toshiba Medical Systems, Tochigi, Japan	Endo VV: 3% Mid VV: 6% Epi VV: 7%
Sarvari et al.	10	Artida;	Artida built-in software;	Endo ICC: 0.81

2013 [15]	Toshiba Medical Systems, Tochigi, Japan	Toshiba Medical Systems, Tochigi, Japan	Mid ICC: 0.84
			Epi ICC: 0.82
Adamu et al. 10	Vivid 7;	EchoPAC;	Endo CS ± SD: 9.9 ± 5.2%
2009 [2]	GE Ultrasound, Horton, Norway	GE Ultrasound, Haifa, Israel	Mid CS ± SD: 9.7 ± 5.1%
			Epi CS ± SD: 10.2 ± 5.1%

CS, variability data on peak systolic circumferential strain; CV: coefficient of variation; Endo: endocardial; Epi: epicardial; ICC: intraclass correlation coefficient;

Mid: mid-myocardial; NA: not available; SD: standard deviation; v: version; VV: variability value.

Table A.3   Interobserver variability in longitudinal layer-specific strain.

Study	*n*	Ultrasound machine; vendor	Software; vendor	Interobserver variability
Shi et al. 2019 [41]	20	Vivid E9; GE Medical Systems, Oslo, Norway	EchoPAC, v 201.x.x; GE Vingmed, Horten, Norway	Endo CV: 5.2 Mid CV: 5.7 Epi CV: 3.2
Iso et al. 2019 [38]	12	Vivid E9; GE Healthcare, Milwaukee, WI, USA	EchoPAC, v 113.1.0; GE Vingmed Ultrasound AS, Horton, Norway	Endo CV: 5.71 Mid CV: 4.88 Epi CV: 4.63
Sun et al. 2019 [17]	20	Vivid E9; GE Healthcare, Horten, Norway	EchoPAC PC, v 113.0.5; GE Healthcare	Endo ICC: 0.92 Mid ICC: 0.93 Epi ICC: 0.93
Xu et al. 2018 [20]	NA	Vivid E9; GE Healthcare, Horten, Norway	EchoPAC PC, v 113.0.5; GE Healthcare	Endo ICC: 0.85 Mid ICC: 0.89 Epi ICC: 0.91
Kang et al. 2018 [10]	10	Vivid E9; GE Healthcare, Horton, Norway	EchoPAC, v 11.1; GE Healthcare, Horton, Norway	Endo ICC: 0.87 Mid ICC: 0.85 Epi ICC: 0.90
Yazaki et al.	12	Vivid E9;	EchoPAC, v 113.1.0;	Endo CV: 2.82

Study	N	Ultrasound system	Analysis software	Results
2018 [22]		GE Healthcare, Milwaukee, WI, USA	GE Vingmed Ultrasound AS, Horton, Norway	Mid CV: 2.13
				Epi CV: 2.44
Tadic et al. 2018 [18]	20	Vivid 7; GE Vingmed, Horten, Norway	EchoPAC, v 201; GE Healthcare, Horten, Norway	Endo ICC: 0.913
				Mid ICC: 0.920
				Epi ICC: 0.811
Yamada et al. 2017 [21]	10	Vivid E7/Vivid E9; GE Healthcare, Milwaukee, WI, USA	EchoPAC, v 113.1.0; GE Vingmed Ultrasound AS, Horton, Norway	Endo CV: 2.26
				Mid CV: 2.13
				Epi CV: 2.57
Leng et al. 2017 [12]	32	Vivid 7; GE Healthcare, Horten, Norway	EchoPAC Dimension 08; GE Healthcare	Endo ICC: 0.929
				Mid ICC: 0.939
				Epi ICC: 0.833
Ejlersen et al. 2017 [8]	20	Vivid 7; GE Healthcare, Horten, Norway	EchoPAC, v 113; GE Vingmed Ultrasound AS, Horton, Norway	Endo MOD ± 95% LOA: 1.35 ± 3.12
				Mid MOD ± 95% LOA: 0.80 ± 2.76
				Epi MOD ± 95% LOA: 0.30 ± 2.59
Cong et al. 2016 [7]	NA	Vivid E9; GE Healthcare, Horten, Norway	EchoPAC PC, v 113.1	Endo MPE[a]: 12.3%
				Mid MPE[a]: 12.8%
				Epi MPE[a]: 12.6%
Hamada et al. 2016 [9]	40	Vivid 7/Vivid E9; GE Vingmed Ultrasound AS, Horten, Norway	EchoPAC v 113.1.0; GE Vingmed Ultrasound AS, Horten, Norway	Endo ICC: 0.91

Kim et al. 2016 [11]	10	ACUSON SC2000; Siemens Medical Solutions, Malvern, PA, USA	Syngo SC2000 Workplace, v 3.0; Siemens Medical Solutions, Malvern, PA, USA	Endo ICC: 0.920 Mid ICC: 0.901 Epi ICC: 0.851
Shi et al. 2016 [4]	20	Vivid E9; GE Medical Systems, Oslo, Norway	EchoPAC, v BT12; GE Vingmed, Horten, Norway	Endo CV ± SD: 5.2 ± 3.8 Mid CV ± SD: 5.7 ± 4.0 Epi CV ± SD: 3.2 ± 3.6
Wang et al. 2016 [19]	10	Vivid 7; GE Healthcare, Waukesha, WI, USA	EchoPAC, v 11.3; GE Healthcare	Endo MOD (95% CI): 0.94% (−2.03 to 1.67%) Mid MOD (95% CI): 0.69% (−1.45 to 1.23%) Epi MOD (95% CI): 0.75% (−1.56 to 1.38%)
Liu et al. 2016 [13]	15	Vivid E9; GE Healthcare, Horten, Norway	EchoPAC, v 113; GE Healthcare, Horten, Norway	Endo ICC: 0.94 Mid ICC: 0.90 Epi ICC: 0.91
Okada et al. 2015 [14]	15	Artida Toshiba Medical Systems, Tochigi, Japan	Artida built-in software; Toshiba Medical Systems, Tochigi, Japan	Endo VV: 13% Mid VV: 12% Epi VV: 22%
Sarvari et al.	10	Artida;	Artida built-in software;	Endo ICC: 0.96

| 2013 [15] | Toshiba Medical Systems, Tochigi, Japan | Toshiba Medical Systems, Tochigi, Japan | Mid ICC: 0.92 |
| | | | Epi ICC: 0.93 |

CI: confidence interval; CV: coefficient of variation; Endo: endocardial; Epi: epicardial; ICC: intraclass correlation coefficient; LOA: limits of agreement; Mid: mid-myocardial; MOD: mean of differences; MPE: mean percentage error; NA: not available; SD: standard deviation; v: version; VV: variability value.

[a] Absolute difference divided by the mean of the two observations.

Table A.4   Interobserver variability in circumferential layer-specific strain.

| Study	n	Ultrasound machine; vendor	Software; vendor	Interobserver variability
Shi et al. 2019 [41]	20	Vivid E9; GE Medical Systems, Oslo, Norway	EchoPAC, v 201.x.x; GE Vingmed, Horten, Norway	Endo CV: 6.0 Mid CV: 8.6 Epi CV: 11.2
Iso et al. 2019 [38]	12	Vivid E9; GE Healthcare, Milwaukee, WI, USA	EchoPAC, v 113.1.0; GE Vingmed Ultrasound AS, Horton, Norway	Endo basal CV: 4.38 Mid basal CV: 3.40 Epi basal CV: 5.86 Endo papillary CV: 4.00 Mid papillary CV: 4.26 Epi papillary CV: 8.95 Endo apical CV: 4.95 Mid apical CV: 4.35 Epi apical CV: 10.15
Sun et al. 2019 [17]	20	Vivid E9; GE Healthcare, Horten, Norway	EchoPAC PC, v 113.0.5; GE Healthcare	Endo ICC: 0.93 Mid ICC: 0.90 Epi ICC: 0.92
Xu et al.	NA	Vivid E9;	EchoPAC PC, v 113.0.5;	Endo ICC: 0.71

2018 [20]		GE Healthcare, Horten, Norway	GE Healthcare	Mid ICC: 0.65
				Epi ICC: 0.73
Kang et al.	10	Vivid E9 ;	EchoPAC, v 11.1;	Endo ICC: 0.91
2018 [10]		GE Healthcare, Horton, Norway	GE Healthcare, Horton, Norway	Mid ICC: 0.83
				Epi ICC: 0.91
Yazaki et al.	12	Vivid E9;	EchoPAC, v 113.1.0;	Endo basal CV: 3.61
2018 [22]		GE Healthcare, Milwaukee, WI, USA	GE Vingmed Ultrasound AS, Horton, Norway	Mid basal CV: 2.69
				Epi basal CV: 6.54
				Endo papillary CV: 2.77
				Mid papillary CV: 2.88
				Epi papillary CV: 4.90
				Endo apical CV: 3.20
				Mid apical CV: 4.40
				Epi apical CV: 5.82
Tadic et al.	20	Vivid 7;	EchoPAC, v 201;	Endo ICC: 0.908
2018 [18]		GE Vingmed, Horten, Norway	GE Healthcare, Horten, Norway	Mid ICC: 0.915
				Epi ICC: 0.805
Yamada et al.	10	Vivid E7/Vivid E9;	EchoPAC, v 113.1.0;	Endo basal CV: 2.12
2017 [21]		GE Healthcare, Milwaukee, WI, USA	GE Vingmed Ultrasound AS, Horton, Norway	Mid basal CV: 2.69

				Epi basal CV: 2.75
				Endo papillary CV: 4.05
				Mid papillary CV: 2.88
				Epi papillary CV: 3.50
				Endo apical CV: 7.42
				Mid apical CV: 4.40
				Epi apical CV: 4.25
Leng et al. 2017 [12]	32	Vivid 7; GE Healthcare, Horten, Norway	EchoPAC Dimension 08; GE Healthcare	Endo ICC: 0.898 Mid ICC: 0.844 Epi ICC: 0.799
Hamada et al. 2016 [9]	40	Vivid 7/Vivid E9 ; GE Vingmed Ultrasound AS, Horten, Norway	EchoPAC, v 113.1.0; GE Vingmed Ultrasound AS, Horten, Norway	Endo ICC: 0.90
Shi et al. 2016 [4]	20	Vivid E9; GE Medical Systems, Oslo, Norway	EchoPAC, v BT12; GE Vingmed, Horten, Norway	Endo CV ± SD: 6.0 ± 4.0 Mid CV ± SD: 8.6 ± 7.6 Epi CV ± SD: 11.2 ± 7.7
Okada et al. 2015 [14]	15	Artida; Toshiba Medical Systems, Tochigi, Japan	Artida built-in software; Toshiba Medical Systems, Tochigi, Japan	Endo VV: 9% Mid VV: 6% Epi VV: 6%
Sarvari et al.	10	Artida;	Artida built-in software;	Endo ICC: 0.84

2013 [15]		Toshiba Medical Systems, Tochigi, Japan	Toshiba Medical Systems, Tochigi, Japan	Mid ICC: 0.81
				Epi ICC: 0.76
Adamu et al.	10	Vivid 7;	EchoPAC;	Endo CS ± SD: 10.8 ± 6.1%
2009 [2]		GE Ultrasound, Horton, Norway	GE Ultrasound, Haifa, Israel	Mid CS ± SD: 10.7 ± 5.9%
				Epi CS ± SD: 10.2 ± 6.2%

CS, variability data on peak systolic circumferential strain; CV: coefficient of variation; Endo: endocardial; Epi: epicardial; ICC: intraclass correlation coefficient; Mid: mid-myocardial; NA: not available; SD: standard deviation; v: version; VV: variability value.

Figure 1.
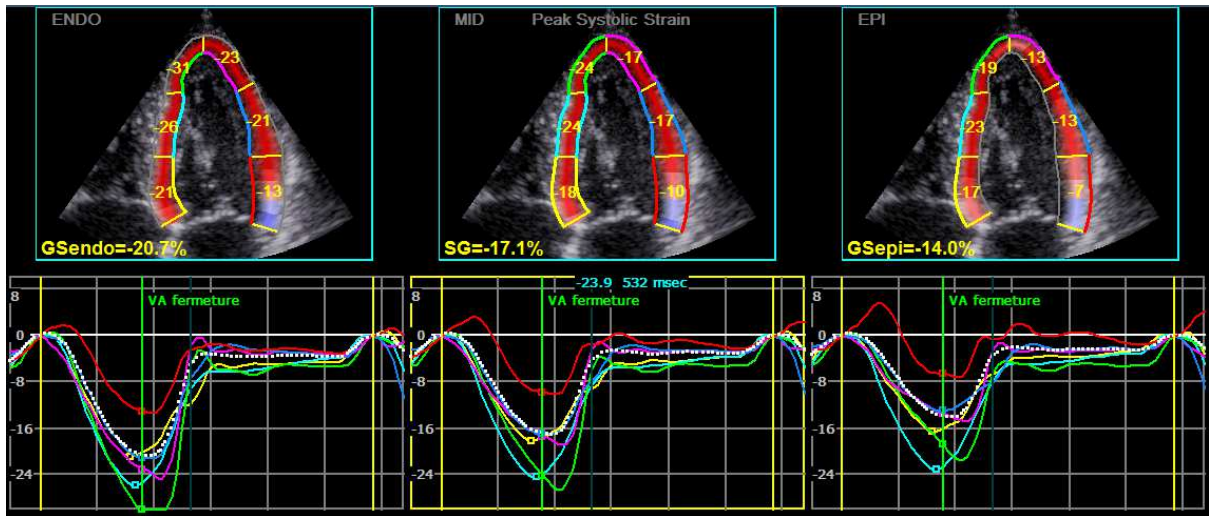
Layer-specific strain using speckle-tracking

Principle :

Using apical 4-, 2- and long-axis views, 2D speckle-tracking echocardiography is performed to analyze longitudinal strain at 3 different LV levels : apex, mid-basal and 3 different LV layers : endocardial, mid-myocardial and epicardial.

Normal values :

- Normal values are not well-defined. Few studies aimed to define normal value.

- Longitudinal LSS decrease from the endocardial to epicardial layer and from apex to base.

Reproducibility :

Intraobserver variability

- When considering longitudinal LSS of endocardial, mid-myocardial and epicardial layers, the ICCs ranged from 0.81 to 0.96, 0.85 to 0.95 and 0.81 to 0.94 respectively.

- When considering circumferential LSS of endocardial, mid-myocardial and epicardial layers,the ICCs ranged from 0.76 to 0.96, 0.77 to 0.95 and 0.81 to 0.97, respectively.

Interobserver variability

- When considering longitudinal LSS of endocardial, mid-myocardial and epicardial layers, the ICCs ranged from 0.82 to 0.96, 0.85 to 0.94 and 0.81 to 0.93, respectively.

- When considering circumferential LSS of endocardial, mid-myocardial and epicardial layers,the ICCs ranged from 0.71 to 0.93, 0.65 to 0.92 and 0.73 to 0.92, respectively.

Causes of variability :

- Age
- Gender
- Heart rate
- Stroke volume
- Intervendor variablility